applied sciences

MDPI

Article

Effect of Excavation Blasting in the Arch Cover Method on Adjacent Existing Pipelines in a Subway Station

Xiang Liu [1], Annan Jiang [1,*], Xinping Guo [1] and Lu Hai [2]

[1] Liaoning Key Laboratory of Marine Environmental Bridge and Tunnel Engineering, Dalian Maritime University, Dalian 116026, China; xliu@dlmu.edu.cn (X.L.); guoxinping113@dlmu.edu.cn (X.G.)
[2] Key Laboratory for Urban Underground Engineering of Ministry of Education, Beijing Jiaotong University, Beijing 100044, China; hailucas@bjtu.edu.cn
* Correspondence: jan20051006@dlmu.edu.cn; Tel.: +86-0411-84724258

Abstract: The dynamic responses of existing pipelines are of great significance to be studied in blasting excavation in the arch cover method. In this paper, the Shi Kui Subway Station Line 5 in Dalian, China, is selected as a case study. A 3D numerical simulation model is established to analyze the dynamics characteristics of the existing pipelines subjected to blasting vibration, with a triangular pattern describing the blast hole pressure. The numerical simulation is verified by comparing the existing pipelines' PPVs of the numerical model and field monitored points. Then, the dynamic responses of the pilot tunnels, existing pipelines, and secondary lining are discussed. The effects of the later pilot tunnel on the earlier pilot tunnel are remarkable when the relative distance between them is small. Extensive blasting areas and many charges will result in large peak velocities of the existing pipelines in a short time, as well as a decreased distance from the pilot tunnels. However, the hollow effect can change these dynamic characteristics. The implementation of a secondary lining can reduce the existing pipelines' dynamic responses when the lower rock is blasted. The most adverse position of the secondary lining is the arch foot rather than the arch crown and arch waist; thus, blasting should be carried out at a suitable age for the concrete to ensure the safety of the structures and pipelines.

Keywords: dynamic responses; excavation blasting; PPV; arch cover method; existing pipelines; numerical simulation

check for updates

Citation: Liu, X.; Jiang, A.; Guo, X.; Hai, L. Effect of Excavation Blasting in the Arch Cover Method on Adjacent Existing Pipelines in a Subway Station. *Appl. Sci.* **2022**, *12*, 1529. https://doi.org/10.3390/app12031529

Academic Editor: Arcady Dyskin

Received: 11 January 2022
Accepted: 27 January 2022
Published: 31 January 2022

1. Introduction

The arch cover method, developed from the traditional shallow tunneling method [1], is widely used to construct subway stations in the upper-soft lower-hard stratum. Due to the low self-stability of soft soil, an upper arch structure in the arch cover method is implemented to allow the bearing capacity of the underlying surrounding rock to be fully utilized. At present, some cities, such as Dalian, Chongqing, and Qingdao in China, have applied the arch cover method to station construction, including two different types of primary lining support and double lining support.

Some scholars [2–7] studied the arch cover method using physical model tests, field measurements, analytical methods, and numerical simulations. The main concerns of the research are tunneling-induced ground deformation, the mechanical responses of the supporting structures, the deformation control effect of various support methods, and the optimal construction sequences. The construction sequences, composed of constructing and dismantling the temporary support, erecting and removing the mid-pillar, setting up the secondary lining, middle plate, and floor, are the critical construction technologies of the arch cover method to control the ground deformation and ensure the safety of subway station.

Nevertheless, the previous research has some drawbacks: (1) Few research study the dynamic responses of the surrounding rock and structures induced by blasting excavation in the arch cover method. (2) The effects of blasting excavation on the existing pipelines have rarely been investigated, considering the complex construction sequences. Although many researchers have widely considered the dynamic responses of blasting on the existing pipelines, few studies have focused on the effects of blasting excavation in the arch cover method.

The dynamic responses of existing pipelines subjected to blasting excavation have been mainly analyzed by means of field tests [8–10], analytical [11–13], and numerical methods [14–16]. Some scholars mainly study the effects of surface blasting on non-pressurized pipelines [17–19]. Subsequently, other scholars began to investigate the dynamic responses of pressurized pipelines, such as gas, water, oil, and steel pipelines [20–24]. Moreover, the dynamic responses of the existing pipelines due to blasting during the construction of adjacent tunnels are studied because it is one of the most detrimental factors for existing pipelines [25]. However, the effects of blasting during different construction sequences of the arch cover method are rarely studied.

This paper aims to study the dynamic responses of the existing pipelines subjected to blasting excavation by the arch cover method. A dynamic geotechnical software Flac3D.5.0 [26] is used to establish a numerical model. A triangular pattern describes the time history of the blast hole pressure. Using the Shi Kui Road Station project, No. 5 Line in Dalian, China, as a case study, our numerical simulation is verified from the monitoring data of the ground vibration in this project. The dynamic response characteristics of the existing pipelines induced by blasting pilot tunnels and the lower rock are analyzed.

2. Engineering Background

2.1. Overview of Subway Station

Shi Kui Subway Station of Dalian Subway Line 5 is located on the north side of the intersection of Jie Fang Road and Shi Kui Road. The subway station is set up as an island station with two layers of underground excavation. The length, width, and height of its main standard section are 235.0 m, 19.9 m, and 20.5 m, respectively. The station is excavated adjacent to various existing structures, such as residential buildings, middle schools, viaducts, and pipelines. Therefore, the adjacent existing structures are so sensitive that high requirements for deformation control are put forward during the construction. A plan view of Shi Kui Subway Station is shown in Figure 1.

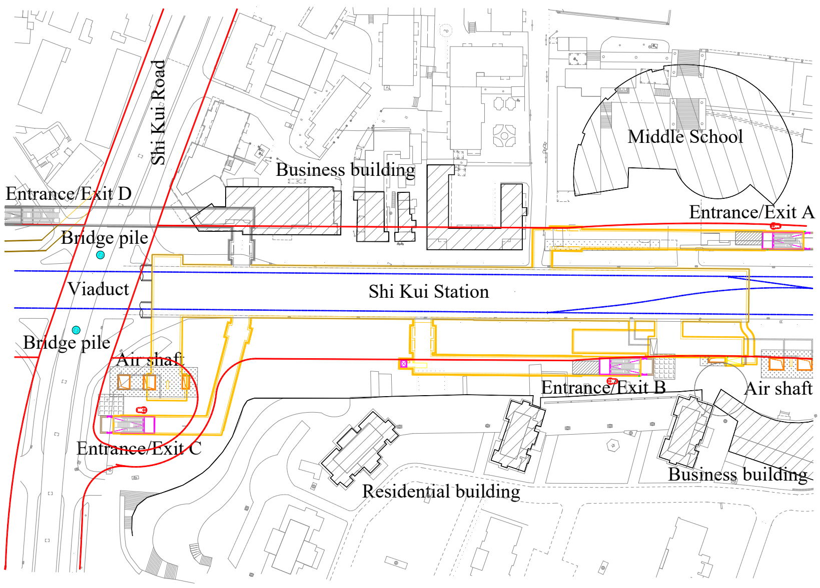

Figure 1. Plan view of Shi Kui Subway Station.

Figure 2 shows the cross-sectional view of the subway station's standard section. The overburden depth of the station is about 11–18 m. The stratum in the station area is composed of plain fill and medium-weathered quartzite, with local inclusions of fully-weathered greywacke and strongly-weathered greywacke. The main body of the station is located in medium-weathered quartzite. Table 1 lists the physical parameters of the rock stratum.

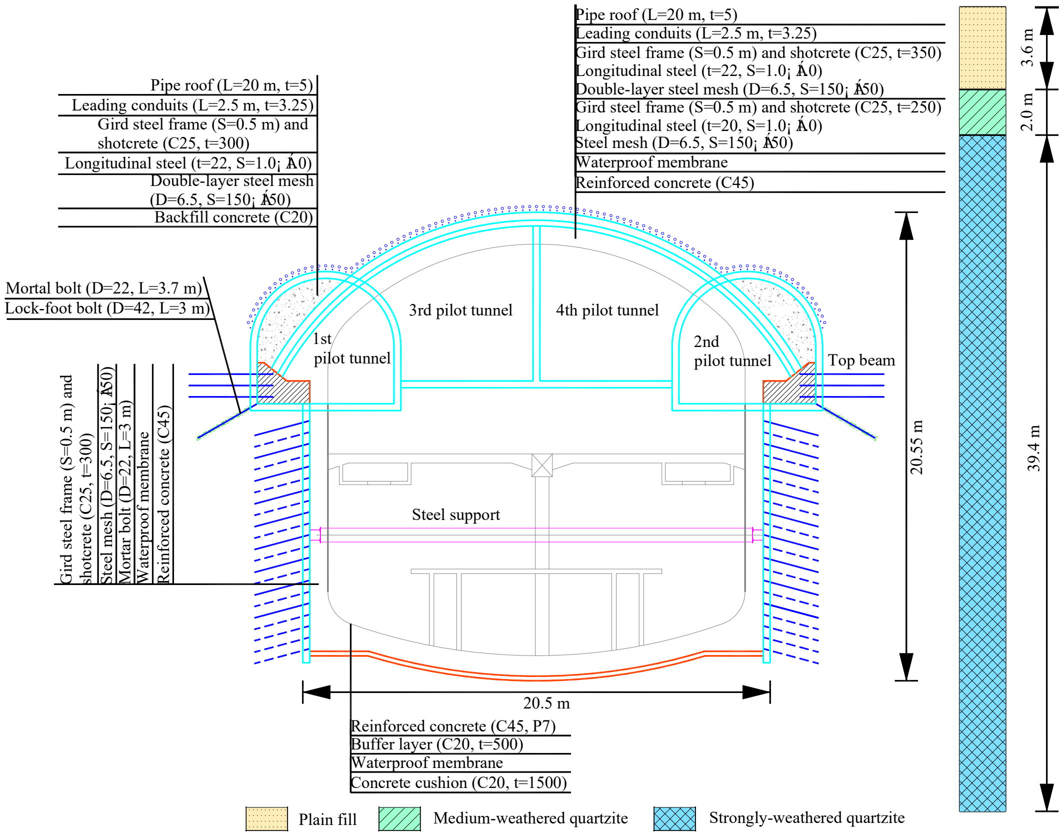

Figure 2. Cross-section view of Shi Kui Subway Station by the arch cover method.

Table 1. Physical parameters of surrounding rock.

Surrounding Rock	Elastic Modulus *E* (MPa)	Poisson' Ratio μ	Bulk Density γ (kNm-3)	Cohesion *c* (kPa)	Friction Angle φ (°)
Plain fill	8	0.40	17	10	15
Strongly-weathered quartzite	50	0.25	23	80	35
Medium-weathered quartzite	1300	0.23	26.5	180	40

2.2. Construction Sequences of Arch Cover Method

To ensure the safety of the adjacent existing structures and to facilitate rock excavation, the subway station is excavated by blasting and the arch cover method. As shown in Figure 2, the station cross-section is excavated respectively in the upper and lower parts, composed of the top arch, sidewall, beam, and slab. Small leading conduits filled with grouting are implemented to pre-reinforce the upper rock mass. The rock mass in the upper part is excavated by four pilot tunnels. After excavating the pilot tunnels, steel frame and shotcrete are carried out. In the pilot tunnels on the left and right sides, top beams are erected and backfilled concrete. The top beam is connected with the side walls. The surrounding rock around the side walls is reinforced with rock bolts. The secondary lining of the upper part is constructed in reverse. After completing the upper part, the rock mass in the lower part is excavated, and the side walls are constructed. Steel supports are set up between the side walls to prevent overturning. The secondary lining of the lower part is constructed in order. W waterproof layer construction is required between the primary support and the secondary lining.

The construction sequences of the arch cover method are shown in Figure 3. The primary construction sequences in detail are as follows:

1. The excavation and primary support for the first and second pilot tunnels are carried out after implementing the grouting reinforcement in advance. Mortar bolts and lock-foot bolts are set up at the foot of the arch cover. The top beams are installed after the first and second pilot tunnels finish;
2. The excavation and primary support are carried out for the third and fourth pilot tunnels. Backfill concrete is filled in the vacant parts of the first and second pilot tunnels;
3. The inner-layer primary support of the arch cover is constructed. Meanwhile, the temporary support in the first and second pilot tunnels is removed;
4. According to the monitored data, the mid-pillar is removed and the secondary lining of the arch is constructed;
5. The lower rock mass is excavated by the bench-cut method. The primary lining and mortar bolts are constructed. The inner steel support is erected. The concrete cushion after excavating to the elevation of the bottom is implemented;
6. The waterproof layer and the secondary lining of the main body are constructed. The internal structure and decoration of the subway station are completed.

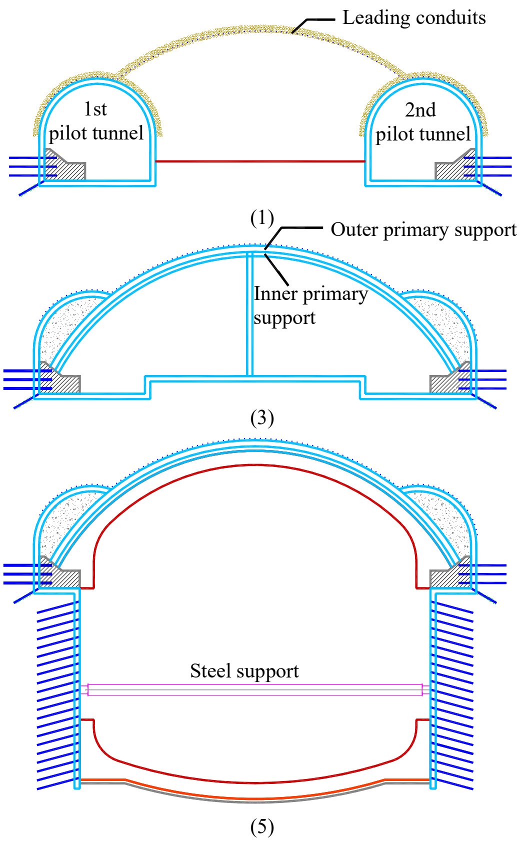

Figure 3. Construction sequences of the arch cover method.

3. Blasting Vibration in the Arch Cover Method

3.1. Design of Blasting

Shi Kui Subway Station is located in a construction site with complex geological conditions adjacent to schools, residential communities, business buildings, and buried gas, water, and sewage pipelines. The blasting vibration induced by blasting excavation of the subway station has a detrimental effect on these existing structures. Thus, the principle of the blasting design is short advancing, slight blasting, strong supporting, and frequent measuring.

Due to the large span of the subway station, the overall blasting excavation of the whole section has a potential safety risk. Blasting excavation is designed in steps. Figure 4 shows the arrangement and partition of the blast holes. The cross-section is divided into eight partitions. The number of blast holes can be calculated by:

$$N = 3.3 \times \sqrt[3]{f \times S^2} \approx 3.3 \times \sqrt[3]{10 \times 411^2} \approx 393 \quad (1)$$

where N is the number of blast holes; f is a firmness factor for rock; S is the cross-sectional area.

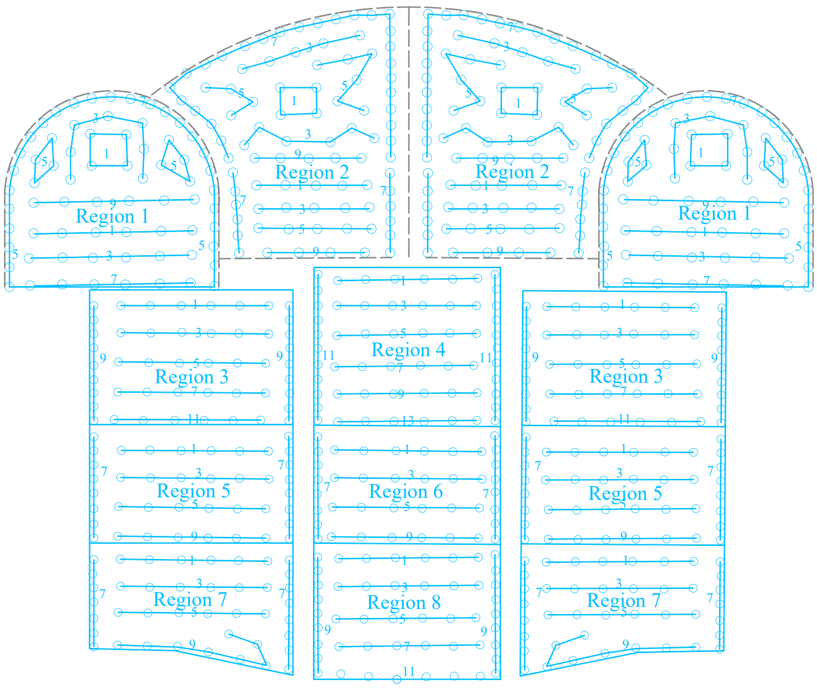

Figure 4. Layout of blast holes.

Blasting excavation speed is adjusted based on the monitoring data and actual geological conditions. The maximum charge weight per delay can be calculated by an empirical solution [27]:

$$Q = R^3 \left(\frac{v}{K}\right)^{\frac{3}{\alpha}} \quad (2)$$

where Q is the charge weight per delay; R is the safe distance from the measurement point to the blast; v is the permissible vibration velocity of safety; K is the propagation coefficient of blast vibration in the medium; α is the attenuation coefficient of blast vibration.

According to the parameters in practice and related regulation [27], the R, v, K, α are set to be 14 m, 1.5 cm/s, 100, and 2.0, respectively. The maximum charge weight per delay is 5.03 kg for this project. The charge, internal, and quantity of individual blast holes can be reasonably adjusted to achieve the optimal blasting effect, considering the geological conditions, the rock fragmentation, and weakness degree.

3.2. Blast Pressure Induced by Rock Blasting

The blast pressure induced by rock blasting follows an exponential attenuation pattern or an approximate triangular pattern. The time history of the blast hole pressure P described by a triangular pattern is straightforward and convenient, as shown in Figure 5. The main parameters are the peak blast pressure P_e, the peak blast pressure rising time t_a, and the vibration period T. Many published papers refer to peak blast pressure attainment time within several milliseconds. However, there are also blast hole measurements that indicate the peak pressure rising time is between 20 and 150 μs, depending on the explosive type and confinement [28].

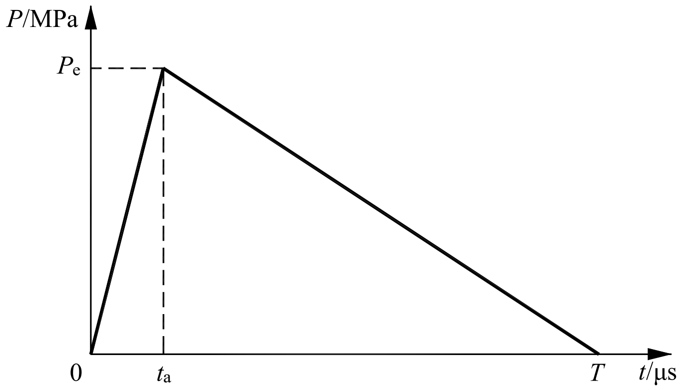

Figure 5. Time history of blast pressure described by triangular pattern.

To estimate the peak blast pressure in the blast wave propagating from a cylindrical explosive, Fickett and Davis [29] and Henrych [30] proposed the following simplified equation derived by the equation of state for an ideal gas:

$$P_d = \rho_e D^2/(1+\gamma) \tag{3}$$

where P_d is the detonation pressure; D is the detonation velocity; ρ_e is the density of the unreacted explosive; γ is the specific heat ratio.

The well-known expression of the detonation pressure for many explosives is given by assuming $\gamma = 3$ [31].

The detonation pressure produces a gas pressure, often called explosion pressure, in the reaction portion of the explosive column. The explosion pressure is exerted on the blast hole walls by expanding gases after the chemical reaction is completed. Ozgur and Tugrul [32] proposed that the explosion pressure is approximately one-half the detonation pressure:

$$P_e = P_d/2 = \rho_e D^2/8 \tag{4}$$

The explosion pressure is also called full coupled blast hole pressure in the case of the charge completely filling the blast hole. However, an empty space exists between an explosive column and the blast hole wall using the decoupling technique. Nie and Olsson [33] provided a calibration equation to consider the decoupling effect.

$$P_0 = P_e(d_c/d_b)^{2\lambda} \tag{5}$$

where d_c is the explosive diameter; d_b is the blast hole diameter; λ is the explosive's adiabatic expansion constant, assuming 1.5 for average adiabatic exponent. Table 2 lists the explosives properties for this project.

Table 2. Explosives properties for this project.

t_a (μs)	T (μs)	P_0 (MPa)	P_e (MPa)	P_d (MPa)	ρ_e (kgm^{-3})	D (m/s)	d_c (mm)	d_b (mm)	a (m)
100	700	133.6	1944	3888	1200	3600	32	40	0.5

3.3. Equivalent Blast Pressure for Numerical Simulation

Applied blast pressures in a numerical simulation are usually categorized into three methods: (a) fluid-structure coupling computation; (b) application of blast pressure–time history curve to the blast hole walls; (c) equivalent blast pressure without considering the blast hole shape. The first two methods require a high level of refinement in the numerical model. Mesh generation is so difficult that large 3D blast vibration simulations are not computable.

Due to the mentioned limits, an equivalent solution of blast pressure acting on the blast hole walls is provided based on St. Venant's principle, and the equivalent blast pressure directly to the blast hole hypocenter line without the mesh generation of the blast hole is applied. Other scholars [34,35] also adopted this method. Figure 6 shows the calculation principle of the equivalent blast pressure. The explosion pressure P_0 is applied to the blast hole wall of d_h diameter. The space of adjacent blast holes is a. The explosion pressure shown in Figure 6a is equated to the equivalent pressures shown in Figure 6b. The expression is:

$$P_E = (d_h/a)P_0 \tag{6}$$

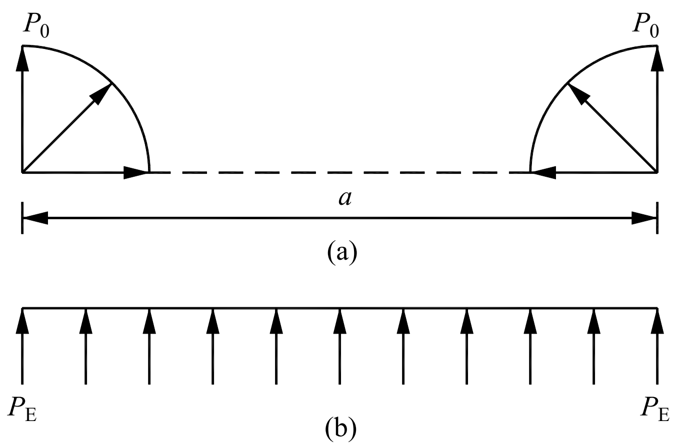

Figure 6. Equivalent blast pressure. (**a**) Explosion pressures; (**b**) Equivalent pressures.

According to the input parameters in Table 2, the equivalent blast pressure P_E is 13.4 MPa. The equivalent blast pressure is applied as a surface pressure onto the normal direction of the tunnel face during the numerical simulation.

4. Verification of Pipeline's Dynamic Response by Numerical Simulation

4.1. Numerical Model

The existing pipeline's dynamic responses induced by the arch cover method and blasting are rarely studied. Buried pipelines are not convenient to monitor and analyze. Thus, we used FLAC3d software to establish a numerical model to study the effects of blasting excavation and the arch cover method on the existing pipeline's dynamic responses. According to Section 3, the equivalent blast pressure of 13.4 MPa was applied as a surface pressure on the normal direction of the excavation face of each arch cover construction sequence. Figure 7 shows the numerical model of the Shi Kui Subway Station.

The overall size of the numerical model was 110 m × 75 m × 18 m. The top of the model was set as a free boundary, whereas the other surfaces were quiet boundaries. The quiet boundary was selected to reduce the reflective waves on the boundary because the explosive pressure was applied inside the numerical model. According to the engineering background in Section 2, the ground is respectively set as plain fill, medium-weathered quartzite, and strongly-weathered quartzite. The mesh generation of the Shi Kui Subway Station was established based on the arch cover method construction sequences in Section 2. The Shi Kui Subway Station is excavated parallel beneath some existing pipelines. The existing pipelines include two water pipelines (DN400, DN900), a drainage pipeline (DN800), and a gas pipeline (DN300). The maximum overburden depth is 3.0 m. The vertical clearances between the pipelines and the station are 12.00 m, 12.47 m, 10.66 m, 12.25 m, respectively. Figure 8 shows the relative location between the pipelines and the subway station. The explosive area is from 1.5 m to 3.0 m along the construction direction.

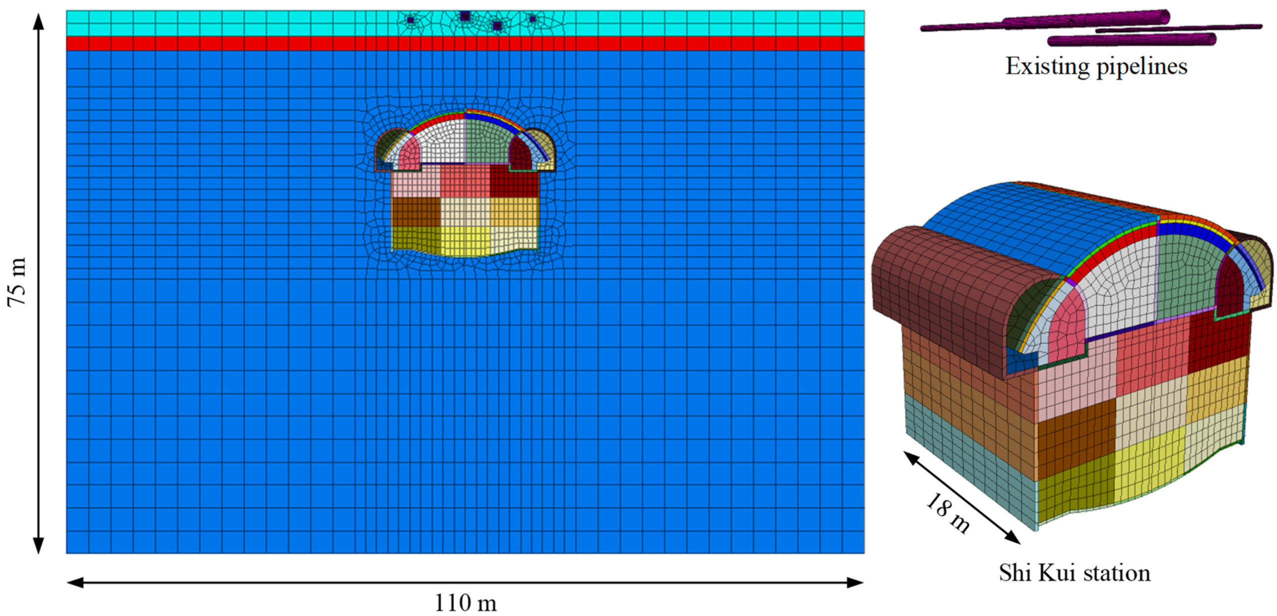

Figure 7. Numerical model of Shi Kui Subway Station.

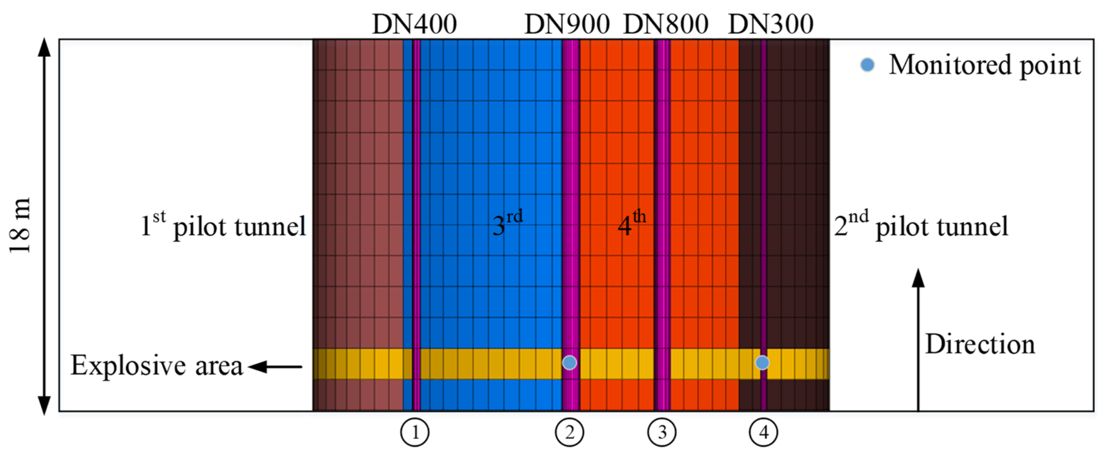

Figure 8. Relative location between pipelines and subway station.

The TC-4850N blasting vibration vibrometers were used to measure blasting excavation in the arch cover method. With a sampling rate of 16 kHz and a monitoring range of 0 to 35 cm/s, the devices can record the vibration velocity versus time curve and easily capture the PPVs of the existing pipelines.

The existing pipelines are not easily accessible for direct monitoring because they are buried in the soil. Therefore, two vibration vibrometers were attached to the ground surface directly above the No. 2 and No. 4 pipelines to obtain the actual vibration velocity. The actual vibration velocity verified our established numerical model.

4.2. Verification of Numerical Model

The monitoring data were selected for comparison to verify the application of the numerical calculation model shown in Figure 8. The subsequent studies on the dynamic responses of the existing pipelines were based on the reliability of the numerical model. Table 3 shows the numerical results of the resultant peak particle velocity (PPV) and the monitored data of each monitored point.

Table 3. Comparison of monitored data and numerical results.

Monitored Point Location	Pilot Tunnel Number	Monitored PPV (cm/s)	Numerical PPV (cm/s)	Relative Difference (%)
④	2nd	0.90	0.94	4.4
②	4th	2.58	2.64	2.3

Figure 9 shows the monitored vibration velocity waveform and the numerical vibration velocity waveform of the ground surface monitored points ④ and ② (directly above the pipelines DN300 and DN800). As shown in Table 3, the PPVs of the monitored points were slightly smaller than those of the numerical simulation. The relative differences of the resultant PPVs were 4.4% and 2.3%, which are less than 10%.

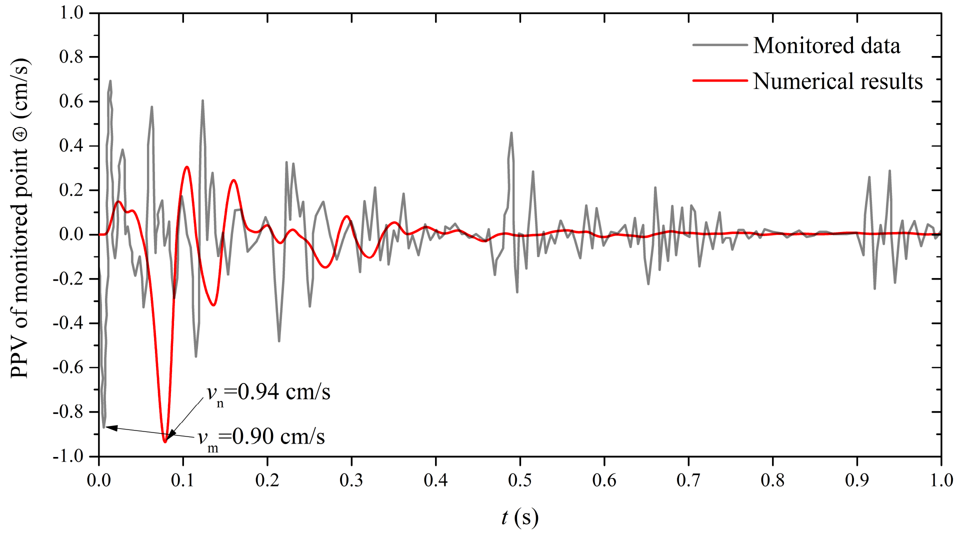

(**a**)

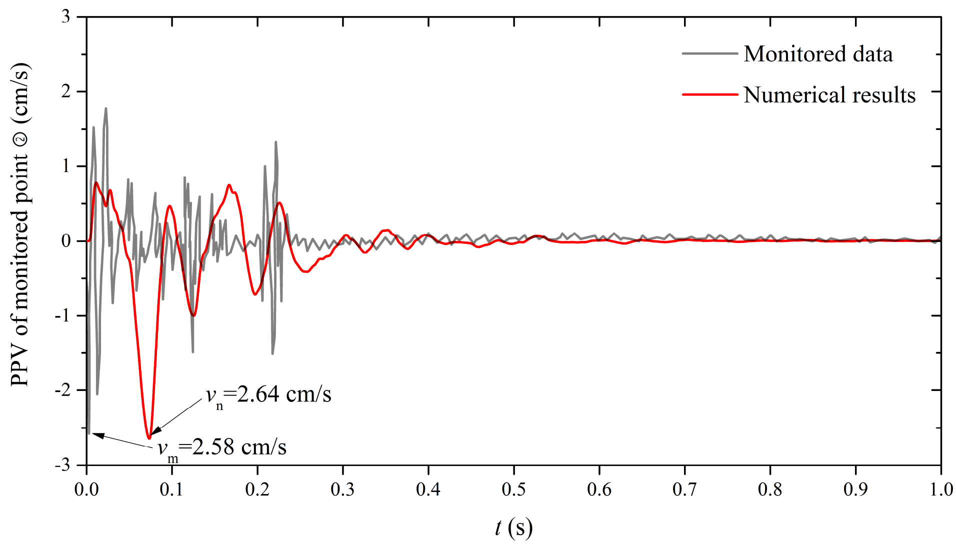

(**b**)

Figure 9. Comparison of vibration velocity waveforms: (**a**) PPV of monitored point ④ induced by the 2nd pilot tunnel; (**b**) PPV of monitored point ② induced by the 4th pilot tunnel.

The numerical waveforms of the vibration velocity were consistent with the monitored ones. The waveform consisted of a large peak in PPV at the beginning and numerous peaks that decayed with time. The vibration period time of the numerical and monitored results was close. The PPV of the numerical model lagged behind that of the monitored points by approximately 0.1 s. It can be attributed to the homogenous simplification of the rock and soil during the numerical simulation. Indeed, soil pores, rock mass joints, and discontinuity in the field delay the propagation of the blast-induced stress waves [36–38].

By comparing the numerical calculation results with the monitored data, the numerical model is applicable, and the model parameters are selected reasonably. The PPVs at each node in the numerical simulation and the field are close. The numerical simulation is used to study the dynamic responses of the existing pipelines because it is impossible to directly monitor the existing pipelines themselves in the actual project.

5. Dynamic Response Characteristics and Safety Analysis

5.1. Dynamic Responses of Earlier Pilot Tunnel Induced by Blasting of Later Pilot Tunnel

In order to study the effect of blasting excavation of the later pilot tunnel on the earlier pilot tunnel and to avoid the influences between adjacent pilot tunnels, the 1st, 2nd, and 4th pilot tunnels were selected for numerical simulation. Figures 10 and 11 show the maximum vibration velocities of the 1st pilot tunnel induced by the blasting of the 2nd pilot tunnel and 4th pilot tunnel, respectively.

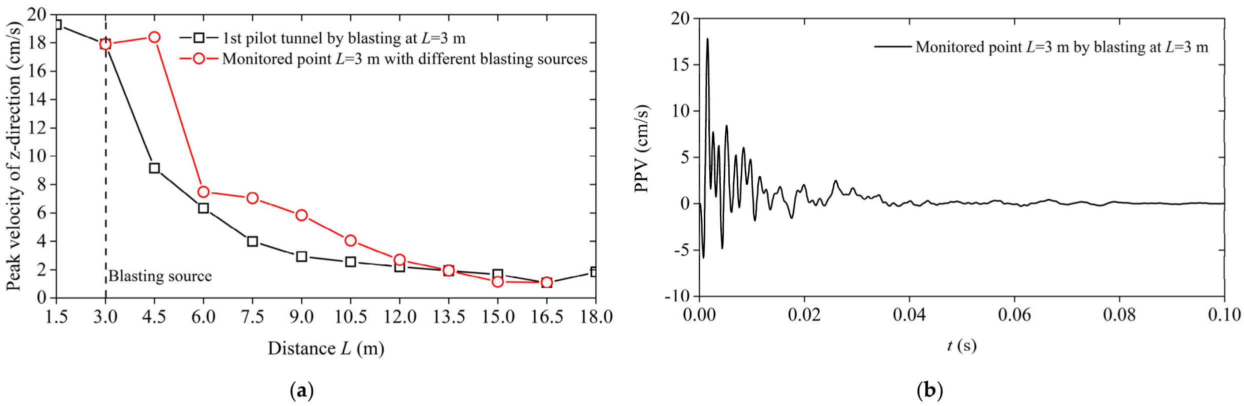

Figure 10. Dynamic responses of the 1st pilot tunnel induced by blasting the 2nd pilot tunnel: (**a**) Peak velocity of x-direction; (**b**) PPV of monitored point L = 3 m.

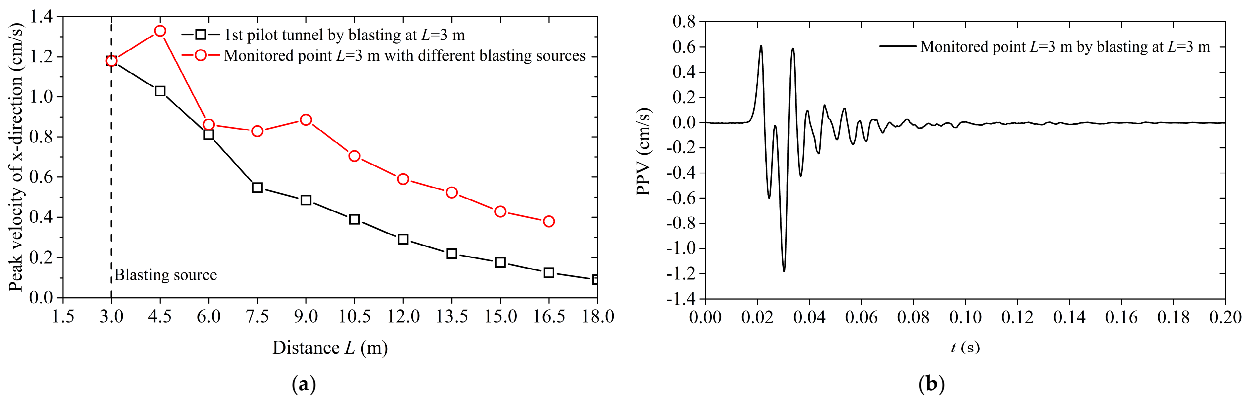

Figure 11. Dynamic responses of the 1st pilot tunnel induced by blasting the 4th pilot tunnel: (**a**) Peak velocity of z-direction; (**b**) PPV of monitored point L = 3 m.

As shown in Figure 10a, the farther away from the blasting source of the 2nd pilot tunnel the monitored point of the 1st pilot tunnel was, the lower peak velocity at the monitored point will be. The peak velocity of the monitored point L = 3 m decreased with the increase in the distance between the monitored point and blasting source. The effects of the 4th pilot tunnel on the 1st pilot tunnel, shown in Figure 11a, were consistent with that of the 2nd pilot tunnel. The maximum peak velocity in Figure 11a was 18.4 cm/s, much larger than 1.34 cm/s in Figure 10a because the 4th pilot tunnel is closer to the 1st pilot tunnel than the 2nd pilot tunnel. Meanwhile, the blasting area and charge of the 4th pilot tunnel were larger. It indicates that the effect of the later pilot tunnel on the earlier pilot tunnel will be more pronounced if the blasting source is closer or the blasting area is more extensive.

Figures 10b and 11b show the PPVs of the 1st pilot tunnel at the minimum blasting distance L = 3 m. The vibration velocity increased to the peak within a relatively short time, gradually attenuated, then eventually stabilized. The velocity of the 1st pilot tunnel peaked at approximately 0.03 s in the case of blasting the 2nd pilot tunnel. However, the peak velocity was reached in less than 0.01 s when the 4th pilot tunnel was blasted. The earlier pilot tunnel will take a shorter time to reach its peak value if the later pilot tunnel's blasting source and blasting area are closer and more extensive.

5.2. Pipeline Dynamic Responses Induced by the Blasting of Pilot Tunnels

Figure 12 shows the pipeline dynamic responses induced by blasting the 1st, 2nd, 3rd, and 4th pilot tunnels, respectively. As shown in Figure 8, the pipelines are directly above the blasting area. The vertical vibration velocities were larger than the horizontal ones. So, we chose the vertical vibration velocity to analyze the dynamic responses. The blasting source was at L = 3 m. The relative distance S is the distance from the monitored points along the pipelines to the blasting source.

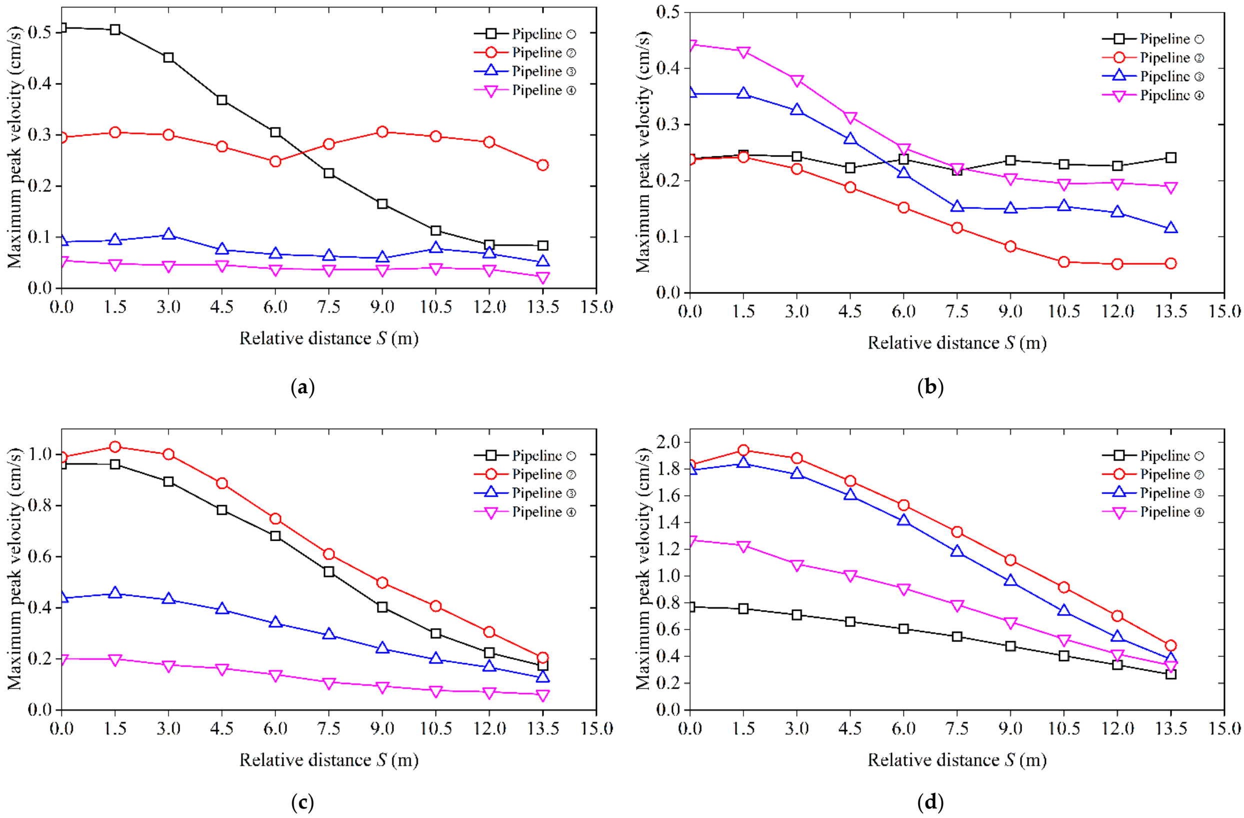

Figure 12. Dynamic responses of existing pipelines induced by blasting the pilot tunnels: (**a**) 1st pilot tunnel; (**b**) 2nd pilot tunnel; (**c**) 3rd pilot tunnel; (**d**) 4th pilot tunnel.

As shown in Figure 12, the maximum peak velocities decreased with the increase in the relative distance S. When the 1st pilot tunnel was blasted, the peak velocities of the pipelines were: $V_{max}^1 > V_{max}^2 > V_{max}^3 > V_{max}^4$ (the superscript is the pipeline number). The dynamic response of pipeline ① decreased remarkably, whereas that of pipeline ②③④ did not. The distance between the 1st pilot tunnel and other pipelines is so far that the effect of blasting on these pipelines was insensitive. When the 2nd pilot tunnel was blasted, the peak velocities were: $V_{max}^4 > V_{max}^3 > V_{max}^1 > V_{max}^2$. The dynamic response of pipeline ① changed little because it is far away from the 2nd pilot tunnel. When the 3rd pilot tunnel was blasted, the peak velocities were: $V_{max}^2 > V_{max}^1 > V_{max}^3 > V_{max}^4$. The changes in the dynamic responses of the pipelines were obvious. Notably, the peak velocity of pipeline ① was much larger than that of pipeline ③, but the pipeline ③ is closer to the blasting source rather than the pipeline ①. It did not conform to the abovementioned characteristics. The reason is that the hollow effect amplifies the pipeline vibration [39]. The 1st pilot tunnel below the pipeline ① had been excavated when the 3rd pilot tunnel blasted. When the 4th pilot tunnel was blasted, the peak velocities were: $V_{max}^2 > V_{max}^3 > V_{max}^4 > V_{max}^1$. The peak velocity of pipeline ② was much larger than that of pipeline ③. The hollow effect of the 3rd pilot tunnel below the pipeline ② also amplified the pipeline vibration.

5.3. Dynamic Responses of Existing Pipelines Induced by Blasting of Lower Rock

According to the construction procedure of the arch cover method, blasting the lower rock is carried out after implementing the secondary lining. The lower rock mass in Region 4 shown in Figure 4 was blasted to study the effects on the existing pipelines. Figure 13 shows the dynamic responses of the existing pipeline ② and ③ induced by blasting the lower rock. The lower rock was first blasted at L = 3 m. The cases with and without the secondary lining of the arch were simulated and compared.

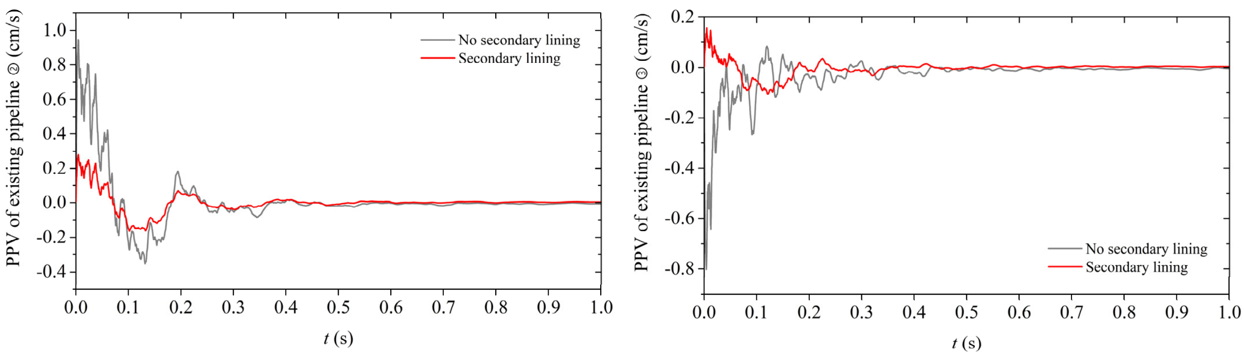

(**a**) (**b**)

Figure 13. Blasting the lower rock with and without secondary lining: (**a**) Existing pipeline ②; (**b**) Existing pipeline ③.

When the secondary lining of the arch was not implemented, the maximum PPVs of the pipeline ② and ③ were about 1.0 cm/s and 0.8 cm/s, respectively. The maximum values were larger than those induced by the 3rd pilot tunnel, smaller than those induced by the 4th pilot tunnel. However, the maximum PPVs of the pipeline ② and ③ decreased to about 0.3 cm/s and 0.15 cm/s when the secondary lining was completed. The results indicate that the secondary lining installation not only controls the deformation but also reduces the effects of blasting on the adjacent structures, such as pipelines and buildings. The prompt implementation of secondary lining is essential for blasting excavation when using the arch cover method.

5.4. Dynamic Responses of Secondary Lining Induced by Blasting the Lower Rock

The dynamic responses of the secondary lining of the arch induced by lower rock blasts require analysis. The blasting of the lower rock mass in the Region 4 was taken as an example to obtain the vertical vibration velocities of the secondary lining. Figure 14 shows the PPVs of the arch crown, arch waist, and arch foot, respectively.

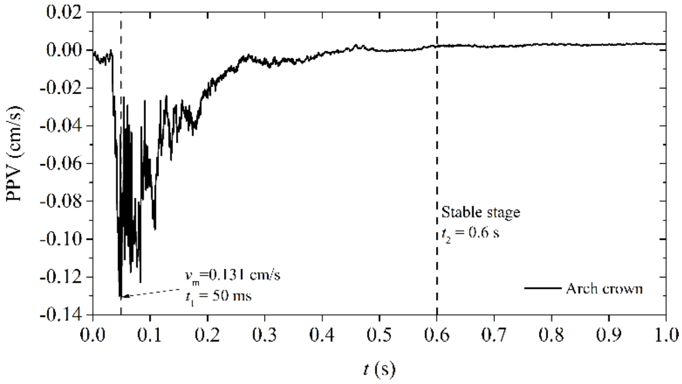

(**a**)

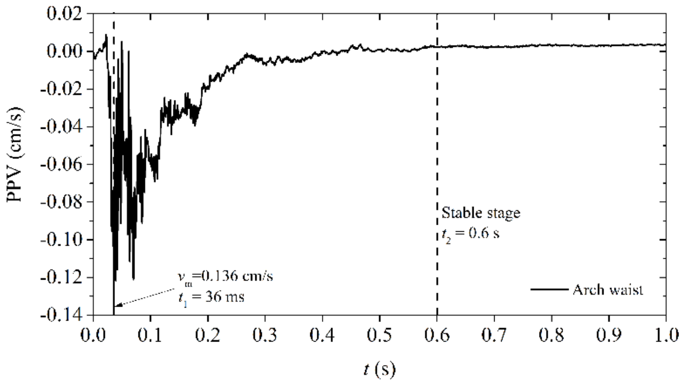

(**b**)

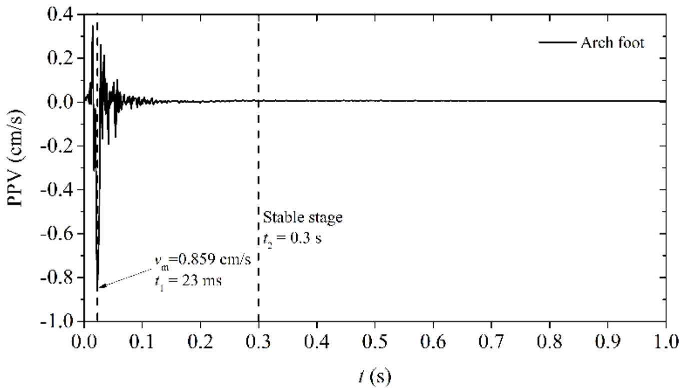

(**c**)

Figure 14. Dynamic responses of secondary lining induced by blasting the lower rock: (**a**) Arch crown; (**b**) Arch waist; (**c**) Arch foot.

As shown in Figure 14, the most adverse position of the secondary lining was the arch foot. The maximum peak velocity was 0.859 cm/s. The vibration velocity of the arch foot peaked at about 23 ms. The PPV was stable after 0.3 s. The maximum peak velocities of the arch crown and arch waist were 0.131 cm/s and 0.136 cm/s, respectively. The peak velocities of the arch crown and arch waist were reached in less than 50 ms and 36 ms. The time required for the velocity stabilization was about 0.6 s. The results indicate that the blast shock wave in the secondary lining mainly propagates through the surrounding rock from near to far. It is essential to take certain protective measures for the arch foot because the arch foot is close to the blasting source of the lower rock.

6. Conclusions

In this paper, four existing pipelines adjacent to the blasting of a subway station were taken as a case study to analyze the dynamic responses induced by the arch cover method. When compared with the ground surface monitoring data, our numerical simulation was verified. The dynamic blasting characteristics of the pilot tunnels, existing pipelines, secondary lining were studied and analyzed. The findings are as follows:

1. When using the arch cover method for construction, the effect of blasting the later pilot tunnel on the earlier pilot tunnel will be pronounced if the clearance between the later and earlier pilot tunnels is smaller. Extensive blasting area and many charges will result in large peak velocity in a short time;
2. The maximum peak velocities of the existing pipelines induced by blasting the pilot tunnels decreased with the increase in the relative distance. The effect of blasting the pilot tunnel on the far pipelines was insensitive. However, the hollow effect can amplify the pipeline vibration to change the characteristics;
3. For blasting in the arch cover method, installing the secondary lining can control the deformation and reduce the effect of blasting on the existing pipelines. Setting up the secondary lining promptly can guarantee the safety of the subway station and adjacent structures;
4. When blasting the lower rock mass, the vibration velocity of the arch foot was larger than that of the arch crown and arch waist. The arch foot is in the most adverse position. The blasting of the lower rock mass should be carried out at a suitable age for the secondary lining concrete, and more attention should be paid to protect the built-up arch structure.

Author Contributions: Conceptualization, X.L. and A.J.; methodology, X.L.; software, X.G.; validation, L.H. and X.G.; formal analysis, X.L.; investigation, X.L.; resources, A.J.; data curation, L.H. and X.G.; writing—original draft preparation, X.L.; writing—review and editing, A.J.; supervision, A.J.; project administration, A.J.; funding acquisition, X.L. All authors have read and agreed to the published version of the manuscript.

Funding: This research was funded by the Chinese National Natural Science Foundation, grant number 52108363 and 52078093, China Postdoctoral Science Foundation, grant number 2021M700654, and LiaoNing Revitalization Talents Program, grant number XLYC1905015.

Institutional Review Board Statement: Not applicable.

Informed Consent Statement: Informed consent was obtained from all subjects involved in the study.

Conflicts of Interest: The authors declare no conflict of interest.

References

1. Fang, Q.; Zhang, D.; Wong, L.N.Y. Shallow tunnelling method (STM) for subway station construction in soft ground. *Tunn. Undergr. Space Technol.* **2012**, *29*, 10–30. [CrossRef]
2. Ji, Z.Q.; Jia, Y.G. Study of Model Tests on Large-Span Tunnel's Damage Caused by Overload with Arch Cover Method. *Adv. Mater. Res.* **2014**, *941–944*, 717–722. [CrossRef]
3. Shang, Y.; Du, S.; Han, T.; Shao, B. Case Study on Deformation Control of Upper-Soft and Lower-Hard Large Span Tunnel Station using Combined Control Technology and Monitoring Demonstration. *Sains Malays.* **2017**, *46*, 2091–2099. [CrossRef]
4. Zhang, G.; Du, Z.; Song, J.; Cai, J.; Tao, T. Monitoring and analysis of excavation-induced subsidence of subway station constructed by arch cover method and control measures. *Chin. J. Rock. Mech. Eng.* **2012**, *31*, 3413–3420. (In Chinese)
5. Song, C.Y.; He, W.G. Structural design of the stacked loaded arch of large-span tunnels in upper-soft lower hard rock stratum. *Modern Tunn. Tech.* **2018**, *55*, 17–26. (In Chinese)
6. Lv, B. Key techniques of the arch-cover method for bored metro stations. *Mod. Tunn. Tech.* **2014**, *51*, 181–187. (In Chinese)
7. Liu, T.; Huang, Y.L.; Lei, G. Analysis of the optimum support dismantling scheme for shallow bored subway stations in a soil-rock compound stratum. *Mod. Tunn. Tech.* **2015**, *52*, 131–137. (In Chinese)
8. Won, J.H.; Kim, M.K.; Kim, G.; Cho, S.H. Blast-induced dynamic response on the interface of a multilayered pipeline. *Struct. Infrastruct. Eng.* **2014**, *10*, 80–92. [CrossRef]
9. Gao, W.; Yan, P.; Li, Z.; Wei, P.; Hou, B. Blasting excavation and vibration effects of shallow tunnel excavation. *Chin. J. Rock Mech. Eng.* **2011**, *30*, 4153–4157. (In Chinese)

10. Wang, H.; Jin, H.; Jia, J. Model test study on the influence of subway tunnel drilling and blasting method on adjacent buried pipeline. *Chin. J. Rock Mech. Eng.* **2018**, *37*, 3332–3339. (In Chinese)
11. Kouretzis, G.P.; Bouckovalas, G.D.; Gantes, C.J. Analytical calculation of blast-induced strains to buried pipelines. *Int. J. Impact Eng.* **2007**, *34*, 1683–1704. [CrossRef]
12. Xia, Y.; Jiang, N.; Zhou, C.; Meng, X.; Luo, X.; Wu, T. Theoretical solution of the vibration response of the buried flexible HDPE pipe under impact load induced by rock blasting. *Soil Dyn. Earthq. Eng.* **2021**, *146*, 106743. [CrossRef]
13. Abedi, A.S.; Hataf, N.; Ghahramani, A. Analytical solution of the dynamic response of buried pipelines under blast wave. *Int. J. Rock Mech. Min. Sci.* **2016**, *88*, 301–306. [CrossRef]
14. Yu, H.; Wang, Z.; Yuan, Y.; Li, W. Numerical analysis of internal blast effects on underground tunnel in soils. *Struct. Infrastruct. Eng.* **2015**, *12*, 1090–1105. [CrossRef]
15. Giannaros, E.; Kotzakolios, T.; Kostopoulos, V. Blast response of composite pipeline structure using finite element techniques. *J. Compos. Mater.* **2016**, *50*, 3459–3476. [CrossRef]
16. Zhang, J.; Zhang, L.; Liang, Z. Buckling failure of a buried pipeline subjected to ground explosions. *Process Saf. Environ. Prot.* **2018**, *114*, 36–47. [CrossRef]
17. Gad, E.F.; Wilson, J.L.; Balendra, T.; Moore, A.J.; Richards, A.B. Response of Pipelines to Blast Loading. *Aust. J. Struct. Eng.* **2007**, *7*, 197–207. [CrossRef]
18. Sohrabi, B.A.; Moradi, A. Consideration of gas pipeline safety against vibration of blasting; Case study: Excavation in Arak-Khorramabad freeway route. *J. Earth Space Phys.* **2017**, *43*, 297–308.
19. Wang, K.; Shi, T.; He, Y.; Li, M.; Qian, X. Case analysis and CFD numerical study on gas explosion and damage processing caused by aging urban subsurface pipeline failures. *Eng. Fail. Anal.* **2019**, *97*, 201–219. [CrossRef]
20. Gospodarikov, A.P.; Kolton, G.A.; Buldakov, E.L. One approach to mathematical modeling of the effect of blast waves on an underground oil pipeline. *Zap. Gorn. Inst.* **2014**, *210*, 37–42.
21. Jiang, N.; Gao, T.; Zhou, C.; Luo, X. Effect of excavation blasting vibration on adjacent buried gas pipeline in a metro tunnel. *Tunn. Undergr. Space Technol.* **2018**, *81*, 590–601. [CrossRef]
22. Jiang, N.; Zhu, B.; He, X.; Zhou, C.; Luo, X.; Wu, T. Safety assessment of buried pressurised gas pipelines subject to blasting vibrations induced by metro foundation pit excavation. *Tunn. Undergr. Space Technol.* **2020**, *102*, 103448. [CrossRef]
23. Zhu, B.; Jiang, N.; Zhou, C.; Luo, X.; Yao, Y.; Wu, T. Dynamic failure behavior of buried cast iron gas pipeline with local external corrosion subjected to blasting vibration. *J. Nat. Gas Sci. Eng.* **2021**, *88*, 103803. [CrossRef]
24. Kakaei, R.; Hajiazizi, M. The effect of GFRP on reinforcing the buried and internally pressurised steel pipes against terrorist attacks. *Int. J. Press. Vessel. Pip.* **2021**, *189*, 104273. [CrossRef]
25. Shi, C.; Zhao, Q.; Lei, M.; Peng, M. Vibration velocity control standard of buried pipeline under blast loading of adjacent tunnel. *Soils Found.* **2019**, *59*, 2195–2205. [CrossRef]
26. Itasca. *FLAC 3D-Fast Lagrangian Analysis of Continua in 3 Dimensions (Version 2.1)*; Itasca Consulting Group Inc.: Minneapolis, MN, USA, 2003.
27. AQSIQ. *Safety Regulations for Blasting*; GB6722-2014; China WaterPower Press: Beijing, China, 2014.
28. Saharan, M.R.; Mitri, H.S.; Jethwa, J.L. Rock fracturing by explosive energy: Review of state-of-the-art. *Fragblast* **2006**, *10*, 61–81. [CrossRef]
29. Fickett, W.; Davis, W.C. *Detonation*; University of California Press: Berkeley, CA, USA, 1979.
30. Henrych, J. *The Dynamics of Explosion and Its Use*; Elsevier Scientific Pub. Co.: Amsterdam, The Netherlands; New York, NY, USA, 1979.
31. Persson, P.-A.; Holmberg, R.; Lee, J. *Rock Blasting and Explosives Engineering*; CRC Press: Boca Raton, FL, USA, 2018.
32. Yilmaz, O.; Unlu, T. Three dimensional numerical rock damage analysis under blasting load. *Tunn. Undergr. Space Technol.* **2012**, *38*, 266–278. [CrossRef]
33. Nie, S.; Olsson, M. Study of fracture mechanism by measuring pressure history in blastholes and crack lengths in rock. In Proceedings of the 27th Annual Conference on Explosives and Blasting Technique, Orlando, FL, USA, 1 February 2000; pp. 291–300.
34. Zhang, Y.C.; Yang, G.H.; Hu, H.Y. Study on numerical model and safety criterion of the influence of blasting vibration on buildings and structures. *China Civ. Eng. J.* **2015**, *48*, 22–29.
35. Zuo, S.Y.; Xiao, M.; Xu, J.K.; Shi, W.B. Numerical simulation of dynamic damage effect of surrounding rocks for tunnels by blasting excavation. *Rock Soil Mech.* **2011**, *32*, 3171–3184.
36. Jiang, Q.; Yang, B.; Yan, F.; Liu, C.; Shi, Y.; Li, L. New method for characterising the shear damage of natural rock joint based on 3D engraving and 3D scanning. *Int. J. Geomech.* **2020**, *20*, 06019022. [CrossRef]
37. Azizabadi, H.R.M.; Mansouri, H.; Fouché, O. Coupling of two methods, waveform superposition and numerical, to model blast vibration effect on slope stability in jointed rock masses. *Comput. Geotech.* **2014**, *61*, 42–49. [CrossRef]
38. Li, J.; Ma, G. Analysis of Blast Wave Interaction with a Rock Joint. *Rock Mech. Rock Eng.* **2010**, *43*, 777–787. [CrossRef]
39. Yu, J.; Liu, S.Y.; Tong, L.Y. Hollow effect induced by blasting vibration in shallow tunnels. *J. Southeast Univ.* **2010**, *40*, 176–179.